ACADÉMIE
DES SCIENCES
INSTITUT DE FRANCE

Comptes Rendus
Chimie

Tian Liu, Yanping Ma, Gregory A. Solan, Jiahao Gao, Qiuyue Zhang, Tongling Liang and Wen-Hua Sun

Effect of chloride substitution on the performance of a benzhydryl-substituted bis(arylimino)pyridyl–cobalt ethylene polymerization catalyst

Volume 28 (2025), p. 771-788

Online since: 24 October 2025

https://doi.org/10.5802/crchim.422

The Comptes Rendus. Chimie *are a member of the Mersenne Center for open scientific publishing*
www.centre-mersenne.org — e-ISSN : 1878-1543

ACADÉMIE DES SCIENCES
INSTITUT DE FRANCE

Comptes Rendus. Chimie
2025, Vol. 28, p. 771-788
https://doi.org/10.5802/crchim.422

Research article

Effect of chloride substitution on the performance of a benzhydryl-substituted bis(arylimino)pyridyl–cobalt ethylene polymerization catalyst

Tian Liu [a,b], Yanping Ma [*,b], Gregory A. Solan [*,b,c], Jiahao Gao [b], Qiuyue Zhang [b], Tongling Liang [b] and Wen-Hua Sun [*,b]

[a] Department of Polyethylene, SINOPEC (Beijing) Research Institute of Chemical Industry Co., Ltd., Beijing, 100013, China

[b] Key Laboratory of Engineering Plastics and Beijing National Laboratory for Molecular Science, Institute of Chemistry, Chinese Academy of Sciences, Beijing 100190, China

[c] Department of Chemistry, University of Leicester, University Road, Leicester LE1 7RH, UK

E-mails: myanping@iccas.ac.cn (Y. Ma), gas8@leicester.ac.uk (G. A. Solan), whsun@iccas.ac.cn (W.-H. Sun)

Abstract. To address the impact of chloride substitution on the performance of a benzhydryl-substituted bis(arylimino)pyridyl–cobalt ethylene polymerization catalyst, this work reports a new family of unsymmetrical N', N, N''-cobalt(II) chloride complexes, **Co1**–**Co5**, incorporating one fixed *N*-2-Me-4,6-bis(4,4′-dichlorodibenzhydryl)phenyl group while the other *N*-aryl group is sterically and electronically variable (aryl = 2,6-dimethylphenyl; 2,6-diethylphenyl; 2,6-diisopropylphenyl; 2,4,6-trimethylphenyl; 2,6-diethyl-4-methylphenyl). Full characterization of all five complexes is supported by representative X-ray structures of **Co1** and **Co2** that display distorted square pyramidal geometries. All cobalt complexes exhibited high activity, under activation with either methylaluminoxane (MAO) or modified MAO (MMAO), with levels reaching up to 14.74×10^6 (g of PE)·(mol of Co)$^{-1}$·h^{-1} at 60 °C producing polyethylene (PE) wax (M_w range: 10.3–34.3 kg·mol^{-1}) with high linearity and narrow dispersity (M_w/M_n range: 2.1–2.5), highlighting their good control. With both aluminum activators, the most sterically demanding cobalt catalyst, **Co3**, afforded the highest molecular weight polyethylene but the lowest catalytic activity.

Keywords. 2,6-Bis(arylimino)pyridine–cobalt complex, *Ortho*-(4,4′-dichlorobenzhydryl) substitution, Ethylene polymerization, High catalytic activity, Narrow dispersity, Linear polyethylene wax.

Funding. Chinese Academy of Sciences (grant no. 2025PVB0034).

Note. Article submitted by invitation.

Manuscript received 7 July 2025, revised 21 August 2025, accepted 10 September 2025.

1. Introduction

Catalysts for ethylene polymerization based on late transition metals have been widely documented since their inception in the mid to late 1990s on account of their exceptional catalytic performance [1–39]. Since these pioneering disclosures, there has been rapid progress in the use of the 2,6-bis(imino)pyridine ligand (A, Chart 1) as a chelating support for both iron and cobalt catalysts, driven

* Corresponding authors

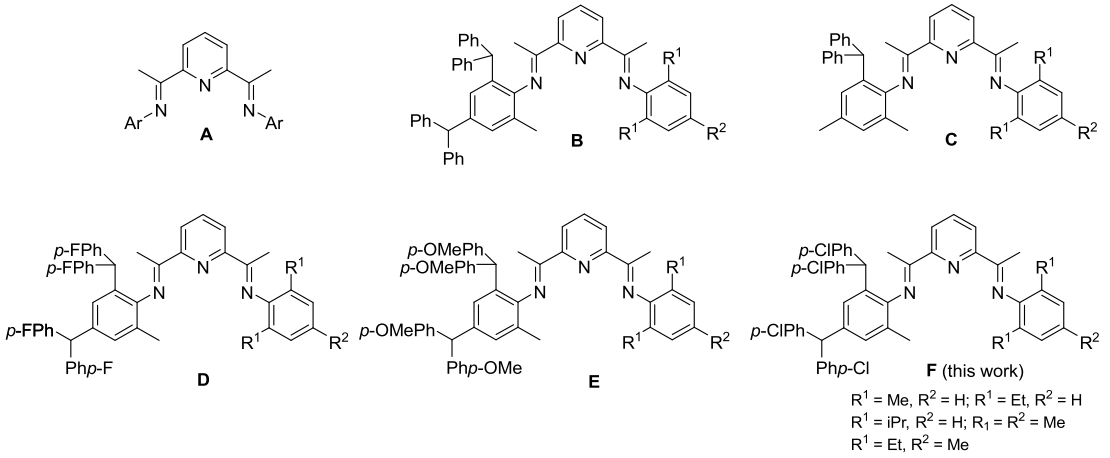

Chart 1. Parent 2,6-bis(arylimino)pyridine (A) and its unsymmetrical derivatives (B–E) incorporating various types of benzhydryl substitution including the subject of this work (F).

by the desire for ever higher activity as well as improvements in thermal stability; recent progress has been reviewed [40,41]. Besides their excellent performance characteristics, such late transition metal catalysts also produce linear polyethylene with a broad range of structural properties that can be modulated by the specifics of the ligand structure [42–46]. Indeed, the resulting polymers offer promise for applications in a variety of fields, such as automobiles, pipes, and so on.

In recent years, our group has been interested in designing new bis(arylimino)pyridyl–iron and –cobalt catalysts by systematically varying the types of *N*-aryl groups [47–50]. Of note, unsymmetrical examples incorporating bulky benzhydryl substitution have emerged including 2,4-dibenzhydryl-6-methylphenyl (B, Chart 1) [47], 2-benzhydryl-4,6-dimethylphenyl (C, Chart 1) [48], 2,4-bis(bis(4-fluorophenyl)methyl)-6-methylphenyl (D, Chart 1) [49] and 2,4-bis(bis(4-methoxyphenyl)methyl)-6-methylphenyl (E, Chart 1) [50]. A notable outcome of these studies is that the *ortho*-benzhydryl substituent can provide protection to the active center and improve thermal stability of the catalyst. Furthermore, the electronic variations made to the periphery of the benzhydryl group (viz., *para*-X = H, F, OMe) can further influence this stability and also affect catalytic activity and various polymer properties.

With the intention of further probing the impact of the benzhydryl's *para*-X group on catalyst activity and polymer properties, we herein focus on the *para*-Cl derivative F (Chart 1) as a support for a cobalt polymerization catalyst. Accordingly, the synthetic details for a family of F are given that encompass a range of steric and electronic variations made to one of the *N*-aryl groups. This set of unsymmetrical N', N, N''-ligands are then used to prepare their cobalt(II) chloride complexes, which are then applied in a comprehensive ethylene polymerization evaluation. The findings of this evaluation are then compared to those reported for cobalt catalysts bearing B–E (Chart 1), with the aim of highlighting any effects of the *para*-Cl substitution on catalytic activity, thermal stability, polymer molecular weight, and dispersity. Full synthetic and characterization data for the complexes, ligands, and polyethylenes are reported.

2. Experimental

2.1. *General considerations*

Standard Schlenk techniques were used in the handling of air- and moisture-sensitive compounds and were conducted under an inert nitrogen atmosphere. Immediately before the polymerization evaluations were conducted, the reaction solvent, toluene, was heated to reflux over sodium and then distilled under nitrogen. High-purity ethylene gas was purchased from Beijing Yansan Petrochemical Co. and used as received. The activators methylaluminoxane (MAO, 1.30 M solution in toluene) and modified methylaluminoxane (MMAO, 1.93 M in *n*-heptane) were

purchased from Anhui Botai Electronic Materials Co. Other reagents were purchased from Aldrich, Acros, or local suppliers (Beijing, China). The ^{1}H and ^{13}C NMR spectra of the organic compounds were recorded on a Bruker DMX 400 MHz instrument at room temperature with TMS as internal standard; chemical shifts are measured in ppm. Elemental analysis was recorded on a Flash EA 1112 micro-analyzer and FT-IR spectra on a System 2000 FT-IR spectrometer. An Agilent PL-GPC 220 GPC instrument was used to determine the molecular weight (M_w) and molecular weight distribution (M_w/M_n) of the resulting polyethylene at 150 °C by using 1,2,4-trichlorobenzene as the eluting solvent. The melting temperatures (T_m) of the polyethylenes were recorded on a PerkinElmer TA-Q2000 differential scanning calorimeter (DSC) under a nitrogen atmosphere. Typically, a sample of about 3.0–5.0 mg was heated up to 160 °C at a rate of 20 °C·min^{-1}, kept for 2 min at 160 °C to delete the thermal history and then cooled at a rate of 20 °C·min^{-1} to −40 °C. The ^{13}C NMR spectra of the polyethylenes were recorded on a Bruker DMX 500 MHz instrument at 100 °C; sample preparation involved a weighed amount of polyethylene (30–50 mg) being dissolved in 1,1,2,2-tetrachloroethane-d_2 with TMS as an internal standard. The imine-ketones, 1-(6-(1-(arylimino)ethyl)pyridin-2-yl)ethan-1-ones (aryl = 2,6-dimethylphenyl; 2,6-diethylphenyl; 2,6-diisopropylphenyl; 2,4,6-trimethylphenyl; 2,6-diethyl-4-methylphenyl) and 2,4-bis(bis(4-chlorophenyl)methyl)-6-methylaniline were prepared as previously described [51,52].

2.2. *Syntheses of 2-{{2,4-((p-ClPh)$_2$CH)$_2$-6-MeC$_6$H$_2$}N=CMe}-6-(ArN=CMe)C$_5$H$_3$N (**L1**–**L5**)*

2.2.1. *Ar: 2,6-Me$_2$C$_6$H$_3$ (**L1**)*

A catalytic amount of *p*-toluenesulfonic acid was added to a solution of 1-(6-(1-((2,6-dimethylphenyl)imino)ethyl) pyridin-2-yl)ethan-1-one (2.54 g, 9.53 mmol) and 2,4-bis(bis(4-chlorophenyl)methyl)-6-methylaniline (5.00 g, 8.66 mmol) in toluene (30 mL). The resulting mixture was stirred and heated under reflux for 9 h. Once cooled to room temperature, the reaction mixture was filtered and all volatile components removed on a rotary evaporator. The remaining solid was loaded onto a basic alumina column and eluted with petroleum ether/ethyl acetate (v/v = 500/1) to afford **L1** as a pale-yellow solid (2.53 g, 35%). ^{1}H NMR (400 MHz, $CDCl_3$, TMS): δ 8.48 (d, J = 8.0 Hz, 1H, Py-H), 8.30 (d, J = 8.0 Hz, 1H, Py-H), 7.90 (t, J = 8.0 Hz, 1H, Py-H), 7.24 (d, J = 8.0 Hz, 4H, Ph-H), 7.16 (d, J = 8.0 Hz, 2H, Ph-H), 7.11–7.08 (m, 4H, Ph-H), 6.96 (d, J = 8.0 Hz, 4H, Ph-H), 6.94 (s, 1H, Ph-H), 6.86 (d, J = 8.0 Hz, 2H, Ph-H), 6.81 (d, J = 8.0 Hz, 3H, Ph-H), 6.38 (s, 1H, Ph-H), 5.35 (s, 1H, –CH–), 5.33 (s, 1H, –CH–), 2.18 (s, 3H, –CH_3), 2.09 (s, 3H, –CH_3), 2.04 (s, 3H, –CH_3), 1.96 (s, 3H, –CH_3), 1.69 (s, 3H, –CH_3). ^{13}C NMR (100 MHz, $CDCl_3$, TMS): δ 168.9, 167.1, 155.3, 154.8, 148.7, 146.8, 142.3, 142.2, 141.3, 140.7, 137.4, 136.8, 132.5, 132.4, 132.4, 132.2, 130.9, 130.6, 130.5, 130.5, 130.5, 129.6, 128.5, 128.3, 128.3, 128.3, 128.0, 127.9, 125.7, 125.4, 123.1, 122.3, 122.0, 55.0, 51.1, 18.0, 17.9, 16.8, 16.4. FT-IR (cm^{-1}): 2917 (w), 1900 (w), 1642 ($\nu_{C=N}$, m), 1594 (w), 1570 (w), 1489 (s), 1466 (m), 1404 (m), 1363 (m), 1297 (w), 1238 (m), 1209 (m), 1121 (m), 1090 (s), 1015 (m), 825 (m), 795 (m), 761 (m), 685 (m). HRMS (MALDI-TOF) m/z: [M]$^-$ Calcd for $C_{50}H_{41}Cl_4N_3$ 823.2049, Found 823.2043. Anal. Calc. for $C_{50}H_{41}Cl_4N_3$ (825.70): C, 72.73; H, 5.01; N, 5.09%, Found: C, 72.23; H, 4.94; N, 4.96%.

2.2.2. *Ar: 2,6-Et$_2$C$_6$H$_3$ (**L2**)*

Using a method and molar ratios of reagents similar to those described for **L1**, **L2** was isolated as a pale-yellow powder (0.36 g, 10%). ^{1}H NMR (400 MHz, $CDCl_3$, TMS): δ 8.46 (d, J = 8.0 Hz, 1H, Py-H), 8.30 (d, J = 8.0 Hz, 1H, Py-H), 7.90 (t, J = 8.0 Hz, 1H, Py-H), 7.24 (d, J = 8.0 Hz, 3H, Ph-H), 7.17 (d, J = 8.0 Hz, 4H, Ph-H), 7.12 (d, J = 8.0 Hz, 4H, Ph-H), 7.05 (s, 1H, Ph-H), 6.97 (d, J = 8.0 Hz, 5H, Ph-H), 6.88 (d, J = 8.0 Hz, 2H, Ph-H), 6.23 (d, J = 8.0 Hz, 3H, Ph-H), 6.40 (s, 1H, Ph-H), 5.36 (s, 1H, –CH–), 5.35 (s, 1H, –CH–), 2.47–2.35 (m, 4H, –CH_2–), 2.21 (s, 3H, –CH_3), 1.97 (s, 3H, –CH_3), 1.71 (s, 3H, –CH_3), 1.20 (t, J = 8.0 Hz, 3H, –CH_3), 1.15 (t, J = 8.0 Hz, 3H, –CH_3). ^{13}C NMR (100 MHz, $CDCl_3$, TMS): δ 169.0, 166.9, 155.3, 154.8, 147.8, 146.8, 142.3, 142.2, 141.3, 140.7, 137.4, 136.8, 132.5, 132.3, 132.2, 131.2, 130.9, 130.5, 130.5, 129.6, 128.5, 128.5, 128.3, 128.3, 126.0, 125.7, 123.4, 122.3, 122.0, 55.0, 51.1, 24.6, 17.9, 16.8, 13.7. FT-IR (cm^{-1}): 2964 (w), 1899 (w), 1640 ($\nu_{C=N}$, m), 1568 (w), 1489 (s), 1452 (m), 1404 (m), 1362 (m), 1296 (w), 1235 (m), 1205 (m), 1120 (m), 1090 (s), 1016 (m), 961 (w), 879 (w), 823 (s), 795 (s), 762 (m), 703 (m),

681 (m). HRMS (MALDI-TOF) m/z: $[M]^-$ Calcd for $C_{52}H_{45}Cl_4N_3$ 851.2362, Found 851.2363. Anal. Calc. for $C_{52}H_{45}Cl_4N_3$ (853.75): C, 73.16; H, 5.31; N, 4.92%, Found: C, 72.85; H, 5.33; N, 4.71%.

2.2.3. *Ar: 2,6-$^i Pr_2C_6H_3$ (**L3**)*

Using a method and molar ratios of reagents similar to those described for **L1**, **L3** was isolated as a pale-yellow powder (0.45 g, 15%). ^{1}H NMR (400 MHz, $CDCl_3$, TMS): δ 8.46 (d, J = 8.0 Hz, 1H, Py-H), 8.30 (d, J = 8.0 Hz, 1H, Py-H), 7.90 (t, J = 8.0 Hz, 1H, Py-H), 7.25–7.09 (m, 13H, Ph-H), 7.04 (d, J = 8.0 Hz, 2H, Ph-H), 7.00–6.95 (m, 3H, Ph-H), 6.88 (d, J = 8.0 Hz, 2H, Ph-H), 6.83 (d, J = 8.0 Hz, 2H, Ph-H), 6.43 (s, 1H, Ph-H), 5.39 (s, 1H, –CH–), 5.34 (s, 1H, –CH–), 2.81–2.69 (m, 2H, –CH–), 2.20 (s, 3H, $-CH_3$), 1.97 (s, 3H, $-CH_3$), 1.71 (s, 3H, $-CH_3$), 1.21 (t, J = 8.0 Hz, 6H, $-CH_3$), 1.17 (t, J = 8.0 Hz, 6H, $-CH_3$). ^{13}C NMR (100 MHz, $CDCl_3$, TMS): δ 170.1, 167.0, 146.4, 145.9, 141.5, 140.7, 136.8, 135.8, 132.3, 132.2, 131.6, 131.0, 130.6, 128.7, 128.6, 128.4, 123.7, 123.0, 122.3, 122.0, 50.9, 28.3, 23.3, 22.9, 21.3, 17.3, 17.1. FT-IR (cm^{-1}): 2960 (w), 1904 (w), 1637 ($\nu_{C=N}$, m), 1569 (w), 1489 (s), 1458 (m), 1405 (w), 1364 (m), 1322 (w), 1305 (w), 1237 (m), 1210 (w), 1124 (m), 1090 (s), 1014 (s), 965 (w), 898 (w), 871 (m), 827 (s), 796 (m), 776 (m), 710 (w), 683 (w). HRMS (MALDI-TOF) m/z: $[M]^-$ Calcd for $C_{54}H_{49}Cl_4N_3$ 879.2675, Found 879.2670. Anal. Calc. for $C_{54}H_{49}Cl_4N_3$ (881.81): C, 73.55; H, 5.60; N, 4.77%, Found: C, 73.75; H, 5.64; N, 4.73%.

2.2.4. *Ar: 2,4,6-$Me_3C_6H_2$ (**L4**)*

Using a method and molar ratios of reagents similar to those described for **L1**, **L4** was isolated as a pale-yellow powder (1.06 g, 15%). ^{1}H NMR (400 MHz, $CDCl_3$, TMS): δ 8.45 (d, J = 8.0 Hz, 1H, Py-H), 8.28 (d, J = 8.0 Hz, 1H, Py-H), 7.89 (t, J = 8.0 Hz, 1H, Py-H), 7.24 (d, J = 8.0 Hz, 4H, Ph-H), 7.18–7.15 (m, 2H, Ph-H), 7.11 (d, J = 8.0 Hz, 2H, Ph-H), 6.96 (d, J = 8.0 Hz, 4H, Ph-H), 6.90 (d, J = 8.0 Hz, 2H, Ph-H), 6.87 (d, J = 8.0 Hz, 2H, Ph-H), 6.81 (d, J = 8.0 Hz, 3H, Ph-H), 6.39 (s, 1H, Ph-H), 5.35 (s, 1H, –CH–), 5.34 (s, 1H, –CH–), 2.31 (s, 3H, $-CH_3$), 2.18 (s, 3H, $-CH_3$), 2.06 (s, 3H, $-CH_3$), 2.01 (s, 3H, $-CH_3$), 1.96 (s, 3H, $-CH_3$), 1.69 (s, 3H, $-CH_3$). ^{13}C NMR (100 MHz, $CDCl_3$, TMS): δ 169.0, 167.3, 155.4, 154.7, 146.8, 146.2, 142.3, 142.2, 141.3, 140.7, 137.4, 136.8, 132.5, 132.3, 132.3, 132.3, 132.2, 130.9, 130.5, 130.5, 130.5, 129.6, 128.6, 128.6, 128.5, 128.5, 128.3, 128.2, 125.7, 125.2, 122.3, 121.9, 55.0, 51.1, 20.7, 17.9, 17.9, 17.8, 16.8, 16.4. FT-IR (cm^{-1}): 2913 (w), 1897 (w), 1640 ($\nu_{C=N}$, m), 1569 (m), 1489 (s), 1403 (m), 1362 (m), 1321 (w), 1239 (w), 1213 (m), 1116 (m), 1088 (s), 1013 (s), 962 (w), 823 (s), 794 (s), 761 (w), 745 (w), 703 (m), 682 (w). HRMS (MALDI-TOF) m/z: $[M]^-$ Calcd for $C_{51}H_{43}Cl_4N_3$ 837.2206, Found 837.2201. Anal. Calc. for $C_{51}H_{43}Cl_4N_3$ (839.73): C, 72.95; H, 5.16; N, 5.00%, Found: C, 73.05; H, 5.17; N, 4.90%.

2.2.5. *Ar: 2,6-Et_2-4-MeC_6H_2 (**L5**)*

Using a method and molar ratios of reagents similar to those described for **L1**, **L5** was isolated as a pale-yellow powder (0.76 g, 17%). ^{1}H NMR (400 MHz, $CDCl_3$, TMS): δ 8.45 (d, J = 8.0 Hz, 1H, Py-H), 8.28 (d, J = 8.0 Hz, 1H, Py-H), 7.89 (t, J = 8.0 Hz, 1H, Py-H), 7.25 (d, J = 8.0 Hz, 6H, Ph-H), 7.17 (d, J = 8.0 Hz, 2H, Ph-H), 7.11 (d, J = 8.0 Hz, 2H, Ph-H), 6.98–6.94 (m, 6H, Ph-H), 6.87 (d, J = 8.0 Hz, 2H, Ph-H), 6.82 (d, J = 8.0 Hz, 3H, Ph-H), 6.39 (s, 1H, Ph-H), 5.36 (s, 1H, –CH–), 5.34 (s, 1H, –CH–), 2.46–2.28 (m, 7H, $-CH_2-$ and $-CH_3$), 2.20 (s, 3H, $-CH_3$), 1.97 (s, 3H, $-CH_3$), 1.71 (s, 3H, $-CH_3$), 1.18 (t, J = 8.0 Hz, 3H, $-CH_3$), 1.13 (t, J = 8.0 Hz, 3H, $-CH_3$). ^{13}C NMR (100 MHz, $CDCl_3$, TMS): δ 169.0, 167.0, 155.4, 154.7, 146.8, 145.2, 142.3, 142.2, 141.3, 140.7, 137.4, 136.8, 132.5, 132.3, 132.3, 132.2, 131.1, 130.9, 130.5, 130.5, 130.5, 129.6, 128.4, 128.3, 128.2, 126.7, 125.7, 122.3, 121.9, 55.0, 51.1, 24.6, 21.0, 17.9, 16.8, 16.7, 13.9, 13.8. FT-IR (cm^{-1}): 2965 (w), 1899 (w), 1642 ($\nu_{C=N}$, m), 1598 (w), 1569 (m), 1489 (s), 1454 (m), 1403 (m), 1365 (m), 1326 (w), 1298 (w), 1257 (m), 1208 (m), 1086 (s), 1013 (s), 865 (m), 823 (m), 795 (s), 745 (m), 709 (w), 681 (w). HRMS (MALDI-TOF) m/z: $[M]^-$ Calcd for $C_{53}H_{47}Cl_4N_3$ 865.2519, Found 865.2513. Anal. Calc. for $C_{53}H_{47}Cl_4N_3$ (867.78): C, 73.36; H, 5.46; N, 4.84%, Found: C, 73.07; H, 5.51; N, 4.76%.

2.3. *Syntheses of [2-{{2,4-((p-ClPh)$_2$CH)$_2$-6-MeC_6H_2}N=CMe}-6-(ArN=CMe)C_5H_3N]$CoCl_2$ (**Co1–Co5**)*

2.3.1. *Ar: 2,6-$Me_2C_6H_3$ (**Co1**)*

Under a nitrogen atmosphere, a Schlenk vessel was loaded with **L1** (0.18 g, 0.22 mmol) and $CoCl_2{\cdot}6H_2O$ (0.047 g, 0.20 mmol) and the contents dissolved in a mixture of freshly distilled dichloromethane (5 mL) and ethanol (10 mL). The reaction mixture was stirred for 9 h at room

temperature after which all volatile components were evaporated under reduced pressure. The remaining residue was dissolved in dichloromethane, and diethyl ether was added to induce precipitation. The precipitate was collected by filtration, washed with diethyl ether, and dried to afford **Co1** as a brown powder (0.17 g, 91%). FT-IR (cm^{-1}): 2915 (w), 2111 (w), 1623 ($\nu_{C=N}$, m), 1589 (m), 1489 (s), 1470 (m), 1439 (w), 1403 (w), 1371 (m), 1261 (m), 1212 (m), 1091(s), 1014 (s), 825 (m), 801 (m), 762 (m), 738 (w), 655 (m). HRMS (ESI) m/z: $[M–Cl]^+$ Calcd for $C_{50}H_{41}Cl_5CoN_3$ 917.1070, Found 917.1070. Anal. Calc. for $C_{50}H_{41}Cl_6CoN_3$ (955.53): C, 62.85; H, 4.33; N, 4.40%, Found: C, 62.52; H, 4.30; N, 4.26%.

2.3.2. *Ar: 2,6-$Et_2C_6H_3$ (**Co2**)*

Using a procedure and molar ratios of reagents similar to those outlined for **Co1**, **Co2** was isolated as a brown powder (0.080 g, 97%). FT-IR (cm^{-1}): 2968 (w), 1903 (w), 1623 ($\nu_{C=N}$, m), 1584 (m), 1489 (s), 1468 (m), 1446 (m), 1404 (w), 1374 (m), 1319 (w), 1263 (m), 1210 (m), 1134 (w), 1088 (s), 1014 (s), 978 (w), 895 (w), 867 (m), 838 (m), 813 (s), 795 (m), 760 (m), 698 (w), 656 (w). HRMS (ESI) m/z: $[M–Cl]^+$ Calcd for $C_{52}H_{45}Cl_5CoN_3$ 945.1383, Found 945.1387. Anal. Calc. for $C_{52}H_{45}Cl_6CoN_3$ (983.59): C, 63.50; H, 4.61; N, 4.27%, Found: C, 63.13; H, 4.59; N, 4.13%.

2.3.3. *Ar: 2,6-$^iPr_2C_6H_3$ (**Co3**)*

Using a procedure and molar ratios of reagents similar to those outlined for **Co1**, **Co3** was isolated as a brown powder (0.070 g, 84%). FT-IR (cm^{-1}): 2964 (w), 1619 ($\nu_{C=N}$, m), 1584 (m), 1489 (s), 1469 (m), 1442 (m), 1404 (w), 1373 (m), 1322 (w), 1263 (m), 1214 (m), 1182 (w), 1090 (s), 1014 (s), 940 (w), 895 (w), 834 (m), 796 (s), 765 (m), 699 (m), 656 (w). HRMS (ESI) m/z: $[M–Cl]^+$ Calcd for $C_{54}H_{49}Cl_5CoN_3$ 973.1696, Found 973.1693. Anal. Calc. for $C_{54}H_{49}Cl_6CoN_3$ (1011.64): C, 64.11; H, 4.88; N, 4.15%, Found: C, 64.03; H, 4.89; N, 4.07%.

2.3.4. *Ar: 2,4,6-$Me_3C_6H_2$ (**Co4**)*

Using a procedure and molar ratios of reagents similar to those outlined for **Co1**, **Co4** was isolated as a brown powder (0.090 g, 87%). FT-IR (cm^{-1}): 2912 (w), 1980 (w), 1618 ($\nu_{C=N}$, m), 1585 (m), 1489 (s), 1403 (m), 1372 (m), 1320 (w), 1264 (m), 1225 (m), 1182 (w), 1090 (s), 1014 (s), 893 (w), 839 (m), 806 (m), 763 (m), 738 (m), 654 (w). HRMS (ESI) m/z: $[M–Cl]^+$ Calcd for $C_{51}H_{43}Cl_5CoN_3$ 931.1226, Found 931.1229. Anal. Calc. for $C_{51}H_{43}Cl_6CoN_3$ (969.56): C, 63.18; H, 4.47; N, 4.33%, Found: C, 62.78; H, 4.48; N, 4.18%.

2.3.5. *Ar: 2,6-Et_2-4-MeC_6H_2 (**Co5**)*

Using a procedure and molar ratios of reagents similar to those outlined for **Co1**, **Co5** was isolated as a brown powder (0.090 g, 87%). FT-IR (cm^{-1}): 2966 (w), 1908 (w), 1622 ($\nu_{C=N}$, m), 1587 (m), 1490 (s), 1465 (m), 1404 (m), 1372 (m), 1322 (w), 1265 (m), 1216 (m), 1182 (w), 1090 (s), 1014 (s), 865 (m), 835 (m), 806 (s), 799 (m), 762 (m), 739 (m). HRMS (ESI) m/z: $[M–Cl]^+$ Calcd for $C_{53}H_{47}Cl_5CoN_3$ 959.1539, Found 959.1540. Anal. Calc. for $C_{53}H_{47}Cl_6CoN_3$ (997.61): C, 63.81; H, 4.75; N, 4.21%, Found: C, 63.30; H, 4.72; N, 4.08%.

2.4. *Polymerization studies*

A 250 mL autoclave, equipped with pressure/temperature control system, mechanical stirrer, and an ethylene cylinder, was employed to conduct the ethylene polymerizations. This autoclave was evacuated and backfilled with nitrogen four times, and then with ethylene gas. The pre-determined amount of cobalt complex (2 μmol) was then added to a dry Schlenk tube (100 mL), which had been evacuated and back-filled with nitrogen three times. Freshly distilled toluene (25 mL) was injected to dissolve the cobalt complex, and the resulting solution transferred quickly to the autoclave. More toluene (25 mL) was injected into the Schlenk tube to dissolve any remaining cobalt complex and added to the previous solution; this was repeated one more time. Once the temperature had reached the required value, the pre-determined amount of activator (MAO or MMAO) was injected into the autoclave with a syringe along with another 25 mL of toluene to take the total volume of solvent to 100 mL. With the ethylene pressure set at 10 atm and the temperature at the pre-identified value (and controlled by circulating water or using a water/ice bath), the reaction was started by stirring at 400 rpm. Once the run time was completed, the reactor was cooled to room temperature, and ethylene pressure vented. The reaction mixture was then quenched using a 5% hydrochloric acid in ethanol solution (100 mL), forming the polyethylene as a white powder. After stirring and washing for 2 h, the polymer was collected using suction filtration and dried in a vacuum oven to a constant weight.

2.5. *X-ray crystallographic studies*

Single-crystal XRD studies on **Co1** and **Co2** were carried out using a XtaLAB Synergy-R diffractometer with mirror-monochromatic Cu-Kα radiation (λ = 1.54184 Å) at 170.00 K; the cell parameters were obtained by global refinement of the positions of all attained reflections. Direct methods were used to solve the structures, and these were refined by full-matrix least-squares on F^2. All hydrogen atoms were placed in calculated positions. Structural solution and refinement were performed using the Olex2 1.2 package and SHELXTL [53]. The application of PLATON software was used during the structural refinement to squeeze the solvent in the lattice [54]. Details of the crystal data and processing parameters are summarized in Table S1.

3. Results and discussion

3.1. *Synthesis and characterization*

Five different examples of 2-[1-(2,4-bis(di(4-chlorophenyl)methyl)-6-methylphenylimino)ethyl]-6-[1-(arylimino)ethyl]pyridine (aryl = 2,6-dimethylphenyl (**L1**); 2,6-diethylphenyl (**L2**); 2,6-diisopropylphenyl (**L3**); 2,4,6-trimethylphenyl (**L4**); 2,6-diethyl-4-methylphenyl (**L5**)) were synthesized by the acid-catalyzed condensation reaction of the corresponding imine-ketone with 2,4-bis(di(4-chlorophenyl)methyl)-6-methylaniline in toluene under reflux; related procedures have been reported elsewhere (Scheme 1) [51]. Compounds **L1**–**L5** were isolated in moderate yield and were characterized by ^{1}H/^{13}C NMR and FT-IR spectroscopy, and purity further confirmed by elemental analysis (see experimental).

Interaction of **L1**–**L5** with $CoCl_2{\cdot}6H_2O$ in a mixture of ethanol and dichloromethane at room temperature afforded, on work-up, **Co1**–**Co5** in excellent yields (Scheme 1). FT-IR spectroscopy proved an effective means of confirming coordination of the N',N,N''-ligands as evidenced by the $\nu_{C=N}$ stretching vibrations of **Co1**–**Co5** shifting to lower wavenumbers (range: 1618–1623 cm^{-1}) when compared with the free ligands (range: 1637–1642 cm^{-1}). In their ESI mass spectra, fragmentation peaks corresponding to [M–Cl]$^+$ ions were seen for all five complexes. Additionally, the elemental analysis data were consistent with elemental compositions based on the general formula $LCoCl_2$. Further confirmation of their composition was provided by the X-ray structures of representative **Co1** and **Co2** (see below).

Table 1. Selected bond lengths (Å) and angles (°) for **Co1** and **Co2**

	Co1	**Co2**
Bond lengths (Å)		
Co(1)–N(1)	2.265(9)	2.211(3)
Co(1)–N(2)	2.051(8)	2.050(3)
Co(1)–N(3)	2.195(9)	2.247(3)
Co(1)–Cl(1)	2.304(3)	2.3070(10)
Co(1)–Cl(2)	2.249(3)	2.2464(9)
Bond angles (°)		
N(1)–Co(1)–N(2)	74.4(3)	74.79(10)
N(1)–Co(1)–N(3)	147.3(3)	144.68(10)
N(2)–Co(1)–N(3)	75.7(3)	74.37(11)
N(1)–Co(1)–Cl(2)	98.1(3)	99.21(7)
N(2)–Co(1)–Cl(2)	141.7(3)	152.57(9)
N(3)–Co(1)–Cl(2)	97.1(2)	100.22(8)
N(1)–Co(1)–Cl(1)	96.7(2)	97.29(7)
N(2)–Co(1)–Cl(1)	103.8(3)	91.86(8)
N(3)–Co(1)–Cl(1)	103.0(3)	100.48(8)
Cl(2)–Co(1)–Cl(1)	114.44(11)	115.54(4)

Single crystals of **Co1** and **Co2** suitable for XRD were obtained by layering a dichloromethane solution of each complex with diethyl ether and leaving the mixture to slowly diffuse at room temperature. Views of **Co1** and **Co2** are shown in Figures 1 and 2, respectively; selected bond lengths and angles for both are collected in Table 1. Both complexes **Co1** and **Co2** are similar and will be discussed together.

In each case, the coordination geometry of the cobalt center can be best described as distorted square pyramidal, with the basal plane defined by N1, N2, N3 and Cl2. The Co1 center sits above the basal plane by 0.571 Å in **Co1** and 0.486 Å in **Co2**, while axial Cl1 further protrudes by 2.853 Å in **Co1** and 2.735 Å in **Co2**. With regard to the Co–N distances, the central Co–$N_{pyridine}$ bond length [2.051(8) (**Co1**), 2.050(3) (**Co2**) Å] is markedly shorter than the exterior Co–N_{imine} ones [2.195(9)–2.265(9) Å], which likely derives from the good donor properties of the central pyridine and the constraints of this N',N,N''-ligand class; similar observations have

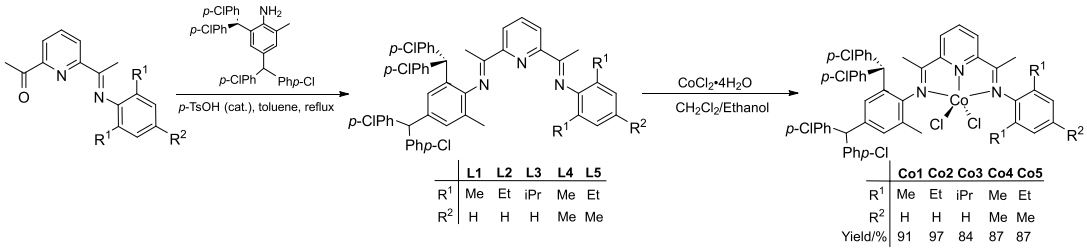

	L1	L2	L3	L4	L5
R^1	Me	Et	iPr	Me	Et
R^2	H	H	H	Me	Me

	Co1	Co2	Co3	Co4	Co5
R^1	Me	Et	iPr	Me	Et
R^2	H	H	H	Me	Me
Yield/%	91	97	84	87	87

Scheme 1. Synthesis of **L1**–**L5** and their use in forming cobalt(II) chloride complexes **Co1**–**Co5**.

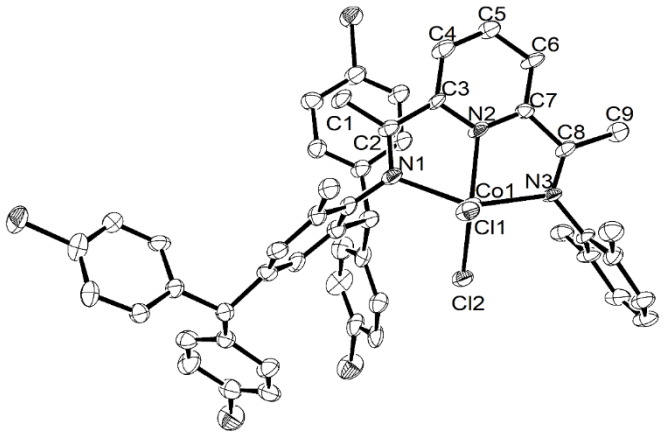

Figure 1. ORTEP representation of **Co1** with the thermal ellipsoids set at the 30% probability level; all hydrogen atoms have been removed for clarity.

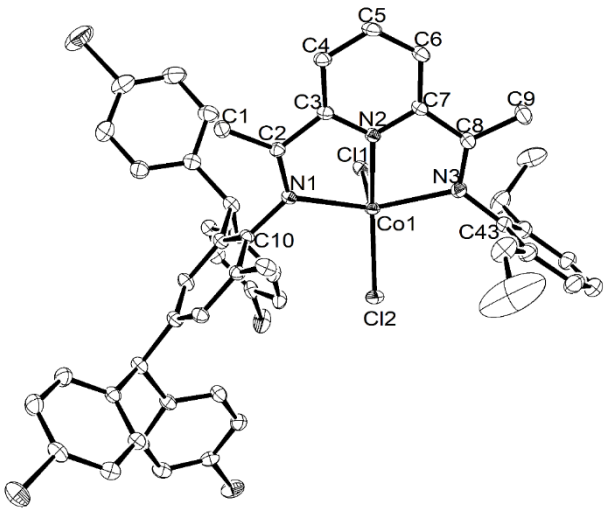

Figure 2. ORTEP representation of **Co2** with the thermal ellipsoids set at the 30% probability level; all hydrogen atoms have been removed for clarity.

been previously noted [51]. The presence of inequivalent *N*-aryl groups causes some more modest variations in the exterior Co–N_{imine} distances, which is also affected by the steric properties exerted by the *N*-2,6-dimethylphenyl (**Co1**) and *N*-2,6-diethylphenyl (**Co2**) groups. In terms of the Co–Cl bond lengths, some variation is also seen with that involving the axial chloride (Co–Cl1: 2.304(3) Å (**Co1**), 2.3070(10) Å (**Co2**)) longer than its basal counterpart (Co1–Cl2: 2.249(3) Å (**Co1**), 2.2464(9) Å (**Co2**)). The *N*-aryl rings are positioned almost perpendicular with respect to the N1–N2–N3–Co1 coordination plane with dihedral angles of 81.61° and 77.03° for **Co1** and 88.74° and 82.63° for **Co2** [52]. There are no intermolecular contacts of note in either structure.

3.2. *Catalytic evaluation for ethylene polymerization*

To explore the performance of **Co1**–**Co5** as precatalysts for ethylene polymerization, side-by-side investigations were conducted using MAO (Table 2) and MMAO (Table 3) as activators. All polymerizations were conducted in toluene with the ethylene pressure initially fixed at 10 atm and the run time at 30 min. Reaction parameters including run temperature, molar ratio of aluminum to cobalt, and reaction time were subject to a systematic investigation. The resulting polyethylenes were characterized by differential scanning calorimetry (DSC) and gel permeation chromatography (GPC). Furthermore, high-temperature ^{13}C NMR spectroscopy was undertaken on selected polyethylene samples in order to provide insight on their microstructural properties. As a matter of course, gas chromatography was performed on post-reaction mixtures which, in all cases, gave no evidence of any oligomeric fractions.

3.2.1. *Evaluation of **Co1**–**Co5**/MAO as ethylene polymerization catalysts*

To pinpoint an effective set of reaction conditions to screen all five complexes with MAO, **Co1** was firstly employed as the test precatalyst to ascertain the optimal temperature, Al:Co molar ratio, and run time. Firstly, with the Al:Co ratio set at 2500, the reaction temperature was changed from 40 to 80 °C (entries 1–5, Table 2), revealing the peak activity of 11.05×10^6 (g of PE)·(mol of Co)$^{-1}$·h^{-1} to occur at 60 °C (entry 3, Table 2). On further increasing the temperature, the level of activity dropped to 2.74×10^6 (g of PE)·(mol of Co)$^{-1}$·h^{-1} at 80 °C (entries 5, Table 2). This finding can likely be accredited to both decomposition of the active species and the lower concentration of ethylene in toluene at higher temperature [55]. Meanwhile, as the reaction temperature increased, the molecular weight of the resulting polyethylene decreased from 16.5 down to 5.3 kg·mol^{-1}, which can be accounted for by a higher rate of chain termination as the temperature was raised. Nevertheless, all polymers generated under these conditions exhibited molecular weights (M_w range: 16.5–5.3 kg mol^{-1}) that can classify them best as polyethylene waxes. The effects of reaction temperature on activity and polymer molecular weight using **Co1**/MAO are further displayed in Figure 3a, while the corresponding GPC traces are collected in Figure 3b.

With the run temperature maintained at the optimal 60 °C, the Al:Co molar ratio using **Co1**/MAO was increased from 1500 to 3500; the results are collected in Table 2 and illustrated in Figure 4. On increasing the ratio, the highest activity of 14.74×10^6 (g of PE)·(mol of Co)$^{-1}$·h^{-1} was achieved with 2000 molar equivalents of MAO (entry 7, Table 2). However, on further raising the Al:Co molar ratio to 3500, the catalytic activity dropped by nearly half to 7.50×10^6 (g of PE)·(mol of Co)$^{-1}$·h^{-1}. In terms of the polymer molecular weight, this remained within a narrow range as the molar ratio was increased, although the slight drop from 11.4 kg·mol^{-1} at 1500 to 10.7 kg·mol^{-1} at 3500 may suggest the onset of some chain transfer from the cobalt to aluminum [56–59].

The influence of reaction time on the polymerization behavior of **Co1**/MAO and the lifetime of the active species was then investigated with the reaction temperature fixed at 60 °C and the Al:Co molar ratio at 2000. Specifically, the tests were run over 5, 15, 30, 45, and 60 min (entries 7 and 10–13, Table 2) and revealed the maximum activity of 32.16×10^6 (g of PE)·(mol of Co)$^{-1}$·h^{-1} to be detected within 5 min (entries 10, Table 2). After this initial spike in activity, the level slowly decreased to only 9.24×10^6 (g of PE)·(mol of Co)$^{-1}$·h^{-1} after 1 h (entry 13, Table 2), which suggests that **Co1**/MAO displayed good stability and appreciable lifetime. Evidently, the active species was quickly generated upon addition of MAO and then underwent a steady deactivation over time [60,61]. As for the polymer molecular

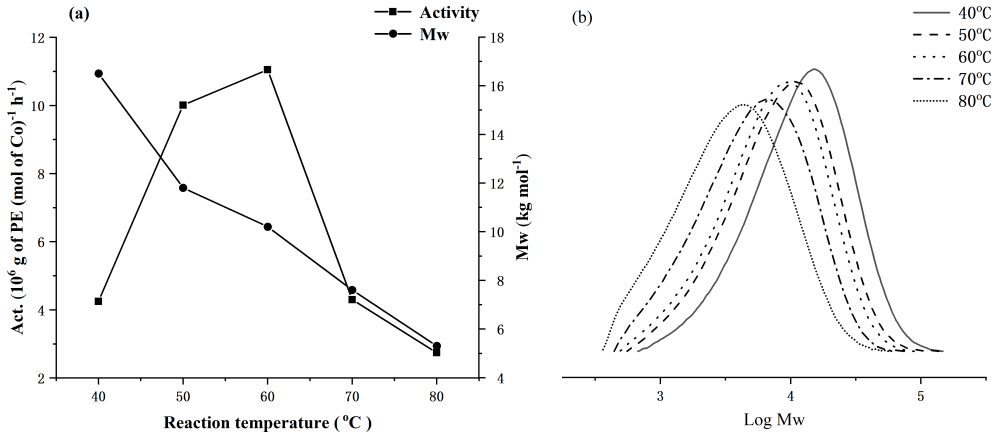

Figure 3. For **Co1**/MAO: (a) dual plots of polymer molecular weight and catalytic activity as a function of run temperature and (b) GPC traces showing variations of log M_w of the polymer as the run temperature is varied (entries 1–5, Table 2).

Table 2. Ethylene polymerization results using **Co1**–**Co5**/MAO at $P_{C_2H_4}$ = 10 atm[a]

Entry	Pre-cat.	T (°C)	Al:Co	t (min)	Mass of PE (g)	Activity[b]	M_w [c] (kg·mol^{-1})	M_w/M_n [c]	T_m [d] (°C)
1	**Co1**	40	2500	30	4.25	4.25	16.5	2.1	135.4
2	**Co1**	50	2500	30	10.01	10.01	11.8	2.2	130.1
3	**Co1**	60	2500	30	11.05	11.05	10.2	2.2	129.7
4	**Co1**	70	2500	30	4.30	4.30	7.6	2.2	129.1
5	**Co1**	80	2500	30	2.74	2.74	5.3	2.2	127.9
6	**Co1**	60	1500	30	8.22	8.22	11.4	2.3	130.5
7	**Co1**	60	2000	30	14.74	14.74	10.4	2.2	130.4
8	**Co1**	60	3000	30	10.51	10.51	10.3	2.2	129.8
9	**Co1**	60	3500	30	7.50	7.50	10.7	2.2	130.1
10	**Co1**	60	2000	5	5.36	32.16	9.5	2.3	129.5
11	**Co1**	60	2000	15	9.96	19.92	10.8	2.1	130.6
12	**Co1**	60	2000	45	16.96	11.31	12.8	2.2	130.1
13	**Co1**	60	2000	60	18.47	9.24	13.7	2.2	130.8
14[e]	**Co1**	60	2000	30	10.21	10.21	9.9	2.3	129.5
15[f]	**Co1**	60	2000	30	0.84	0.84	6.4	2.4	127.8
16	**Co2**	60	2000	30	12.57	12.57	18.6	2.3	131.4
17	**Co3**	60	2000	30	8.55	8.55	34.2	2.1	131.6
18	**Co4**	60	2000	30	14.60	14.60	13.0	2.2	130.3
19	**Co5**	60	2000	30	9.34	9.34	20.4	2.2	131.5

[a]Reaction conditions: 2.0 μmol of cobalt precatalyst, 100 mL toluene, 10 atm ethylene; [b]10^6 (g of PE)·(mol of Co)$^{-1}$·h^{-1}; [c]measured using GPC; [d]measured using DSC; [e]ethylene pressure = 5 atm; [f]ethylene pressure = 1 atm.

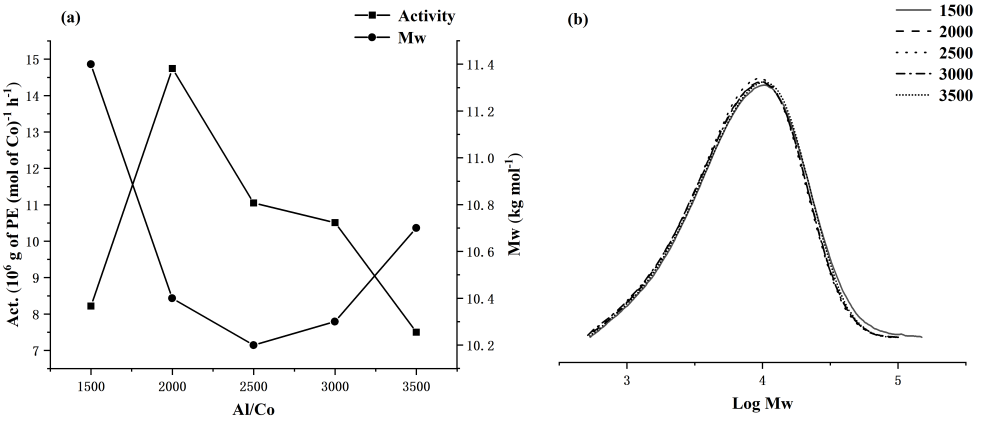

Figure 4. For **Co1**/MAO: (a) dual plots of polymer molecular weight and catalytic activity as a function of Al:Co molar ratio and (b) GPC traces showing the modest effect of Al:Co molar ratio on log M_w (entries 3 and 6–9, Table 2).

Table 3. Ethylene polymerization results using **Co1**–**Co5**/MMAO at $P_{C_2H_4}$ = 10 atm[a]

Entry	Precat	T (°C)	Al:Co	t (min)	Mass of PE (g)	Activity[b]	M_w[c] (kg·mol^{-1})	M_w/M_n[c]	T_m[d] (°C)
1	**Co1**	20	2500	30	3.50	3.50	38.7	2.2	132.8
2	**Co1**	30	2500	30	3.93	3.93	27.8	2.3	132.2
3	**Co1**	40	2500	30	2.68	2.68	17.3	2.3	130.7
4	**Co1**	50	2500	30	1.82	1.82	14.2	2.4	130.3
5	**Co1**	60	2500	30	1.59	1.59	13.5	2.4	130.0
6	**Co1**	30	2000	30	3.25	3.25	29.3	2.4	131.7
7	**Co1**	30	3000	30	4.55	4.55	31.5	2.3	132.0
8	**Co1**	30	3500	30	3.58	3.58	29.7	2.4	132.2
9	**Co1**	30	4000	30	3.24	3.24	29.0	2.2	132.0
10	**Co1**	30	3000	5	2.29	13.74	29.4	2.5	132.0
11	**Co1**	30	3000	15	2.88	4.32	29.7	2.3	131.9
12	**Co1**	30	3000	45	5.39	3.59	31.9	2.2	132.3
13	**Co1**	30	3000	60	5.87	2.94	33.0	2.2	132.0
14[e]	**Co1**	30	3000	30	2.91	2.91	29.6	2.3	132.4
15[f]	**Co1**	30	3000	30	1.05	1.05	29.4	2.4	131.8
16	**Co2**	30	3000	30	3.55	3.55	29.6	2.3	133.3
17	**Co3**	30	3000	30	3.32	3.32	32.0	2.3	133.9
18	**Co4**	30	3000	30	4.07	4.07	30.6	2.1	132.4
19	**Co5**	30	3000	30	3.35	3.35	30.1	2.1	133.3

[a]Reaction conditions: 2.0 μmol of cobalt precatalyst, 100 mL toluene, 10 atm ethylene; [b]10^6 (g of PE)·(mol of Co)$^{-1}$·h^{-1}; [c]measured using GPC; [d]measured using DSC; [e]ethylene pressure = 5 atm; [f]ethylene pressure = 1 atm.

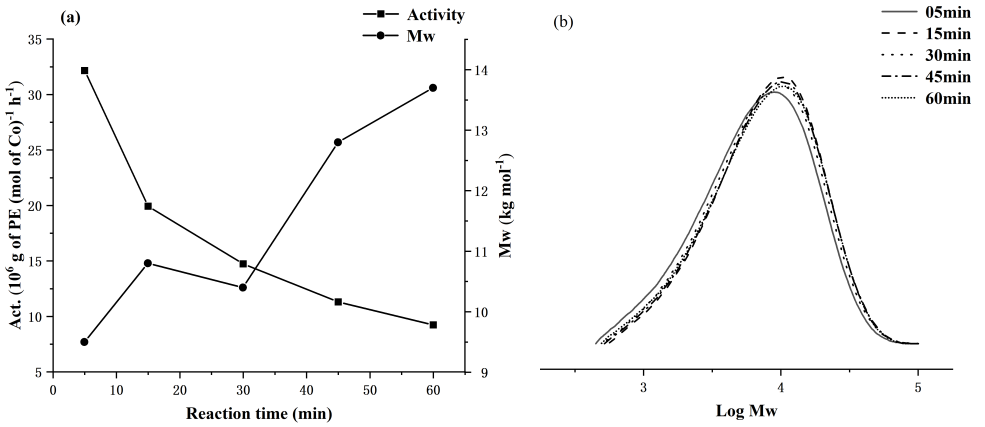

Figure 5. For **Co1**/MAO: (a) dual plots of polymer molecular weight and catalytic activity as a function of run time and (b) GPC traces showing the effect of run time on log M_w of the polymer (entries 7 and 10–13, Table 2).

weight, this was found to slowly increase over reaction time (Figure 5), which demonstrated that the active species remained potent throughout [62,63].

With the optimum polymerization conditions established for **Co1**/MAO as 60 °C (run temperature), 2000 (Al:Co molar ratio), and 30 min (run time), **Co2**–**Co5** were then investigated similarly (entries 16–19, Table 2). All precatalysts exhibited high activity and thermal stability with the activity falling in the order: **Co1** (2,6-di(Me)) > **Co4** (2,4,6-tri(Me)) > **Co2** (2,6-di(Et)) > **Co5** (2,6-di(Et)-4-Me) > **Co3** (2,6-di(^{i}Pr)). Evidently, the steric properties of the precatalyst affect the performance with more sterically bulky *ortho*-groups impeding coordination and insertion of ethylene, resulting in lower activity [56]. By contrast, the bulkiest precatalyst **Co3** afforded the polymer exhibiting the highest molecular weight (34.2 kg·mol^{-1}, entry 17, Table 2) of the series, where the steric properties have the additional role of hindering chain termination pathways leading to polyethylene of relatively high molecular weight [57]. The effects of precatalyst type on activity and polymer molecular weight are further displayed in Figure 6a, while the corresponding GPC traces are collected in Figure 6b.

3.2.2. *Evaluation of **Co1**–**Co5**/MMAO as ethylene polymerization catalysts*

With MMAO now employed as the activator, **Co1** was again employed to optimize the conditions of the polymerization. As with MAO, this initial study focused on the effects of run temperature, Al:Co molar ratio, and reaction time; the complete set of results are gathered in Table 3. With the Al:Co molar ratio firstly set at 2500, the polymerization temperature was increased from 20 to 60 °C (entries 1–5, Table 3). In this case, the highest activity of 3.93×10^6 (g of PE)·(mol of Co)$^{-1}$·h^{-1} was observed at 30 °C rather than 60 °C as with MAO, highlighting the importance of the activator on the active catalyst's temperature stability. With regard to the polyethylene, molecular weights gradually lowered as the reaction temperature was increased (Figure 7), which can be accounted for by the faster chain termination at higher temperature [52]. In comparison with the results obtained using MAO, the polyethylenes produced using **Co1**/MMAO generally showed slightly higher molecular weights but possessed similarly narrow dispersities ($M_w/M_n \leq 2.4$). Additionally, **Co1**/MMAO showed in general lower catalytic activities, which could plausibly derive from the differences between MMAO and MAO, and their effects on the active species.

Next, the Al:Co molar ratio using **Co1**/MMAO was altered with the run temperature maintained at 30 °C (entries 2 and 6–9, Table 3) leading to the highest activity of 4.55×10^6 (g of PE)·(mol of Co)$^{-1}$·h^{-1} being achieved with a ratio of 3000 (entry 7, Table 3). As with **Co1**/MAO, the catalytic activity gradually declined at higher ratios, while polymer molecular weight remained relatively constant (M_w range: 27.8–31.5 kg mol^{-1}) but with a perceptible decrease especially at higher ratios.

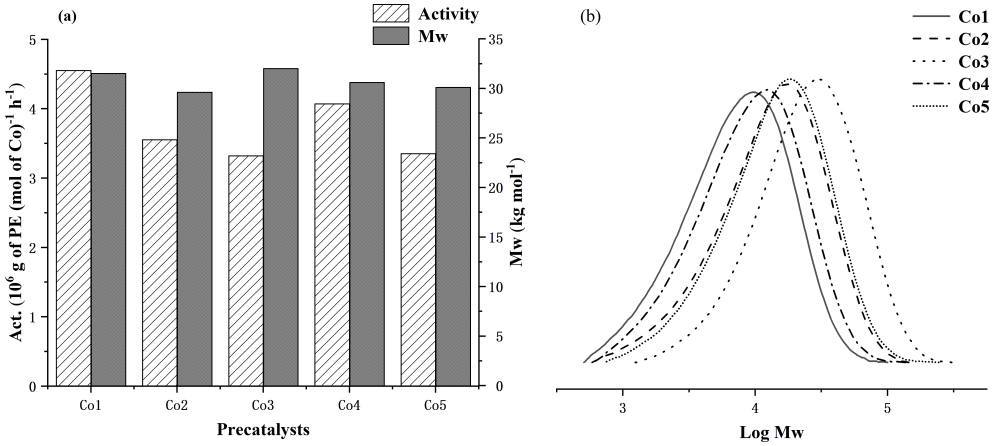

Figure 6. (a) Bar chart displaying catalytic activity and polymer molecular weight with respect to the cobalt precatalyst and (b) GPC traces showing log M_w as a function of the precatalyst (entries 7 and 16–19, Table 2); all runs conducted with MAO as activator at $P_{C_2H_4}$ = 10 atm.

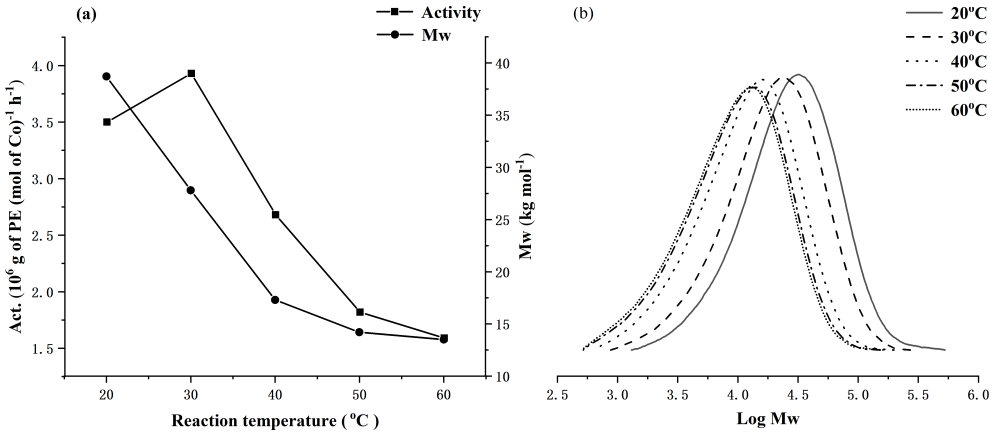

Figure 7. For **Co1**/MMAO: (a) dual plots of polymer molecular weight and catalytic activity as a function of run temperature and (b) GPC traces showing the effect of run temperature on the log M_w of the polymer (entries 1–5, Table 3).

On modifying the reaction time from 5 to 60 min (entries 7 and 10–13, Table 3), the activity of **Co1**/MMAO reached a maximum of 13.74×10^6 (g of PE)·(mol of Co)$^{-1}$·h^{-1} after 5 min and then revealed a gradual decrease to 2.94×10^6 (g of PE)·(mol of Co)$^{-1}$·h^{-1} after 60 min, a finding suggesting that the active species was formed quickly but then underwent deactivation as time elapsed [58]. The effect of ethylene pressure was also explored, with the activity of **Co1**/MMAO found to fall as the pressure was lowered from 10 atm (4.55×10^6 (g of PE)·(mol of Co)$^{-1}$·h^{-1}; entry 7) to 5 atm (2.91×10^6 (g of PE)·(mol of Co)$^{-1}$·h^{-1}; entry 14) to 1 atm (1.05×10^6 (g of PE)·(mol of Co)$^{-1}$·h^{-1}; entry 15); similar effects were seen with MAO and reflect the importance of ethylene pressure to chain propagation in these systems.

With the optimal conditions for **Co1**/MMAO now in place (run temperature = 30 °C, Al:Co molar ratio = 3000), the remaining precatalysts **Co2**–**Co5** were evaluated accordingly. In terms of catalytic activity, the trend essentially mimics that seen with MAO: **Co1** (2,6-di(Me)) > **Co4** (2,4,6-tri(Me)) > **Co2** (2,6-di(Et)) > **Co5** (2,6-di(Et)-4-Me) ~ **Co3** (2,6-di(^{i}Pr)). Again, the *ortho*-methyl precatalysts **Co1** and **Co4** exhibit higher catalytic activity than their bulkier *ortho*-ethyl or *ortho*-isopropyl counterparts (**Co2**, **Co3**, **Co5**); this

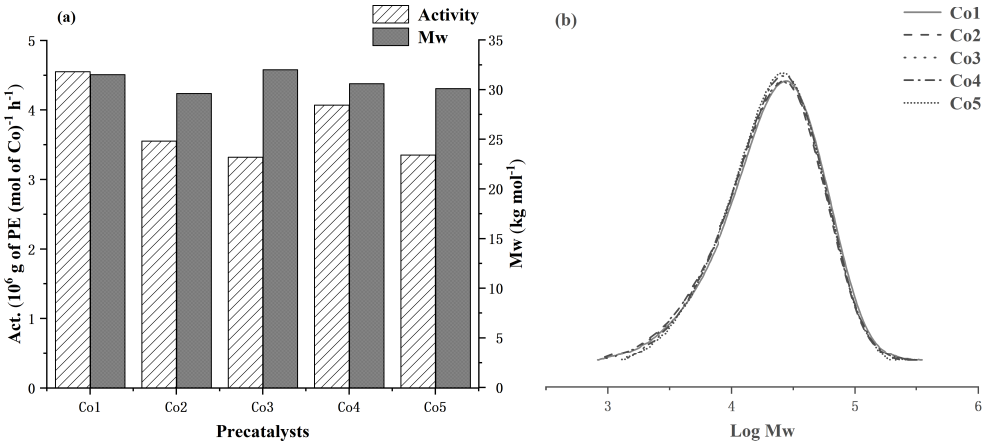

Figure 8. (a) Bar chart displaying catalytic activity and molecular weight of the polymer with respect to the cobalt precatalyst and (b) GPC traces showing log M_w as a function of the precatalyst (entries 7 and 16–20, Table 3); all runs performed using MMAO as activator and $P_{C_2H_4}$ = 10 atm.

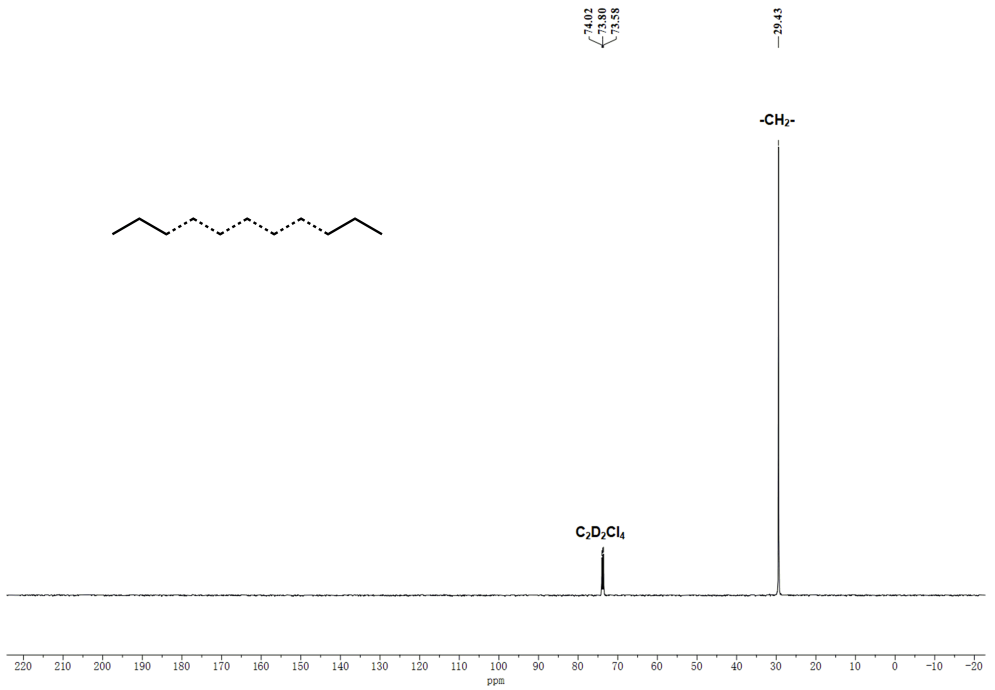

Figure 9. ^{13}C NMR spectrum of the PE sample produced using **Co1**/MAO as catalyst at 60 °C (entry 7, Table 2); recorded at 100 °C in 1,1,2,2-tetrachloroethane-d_2.

observation is consistent with that observed with MAO. In all cases, the dispersity of the polyethylene is narrow (M_w/M_n range: 2.4–2.1), which is also borne out in the GPC traces (Figure 8), which supports the single-site-like nature of the active species.

3.3. *Microstructural analysis of the polyethylenes*

As can be gathered from Tables 2 and 3, all polyethylenes display melting temperatures (T_m) in excess of 127 °C, values that are typical of

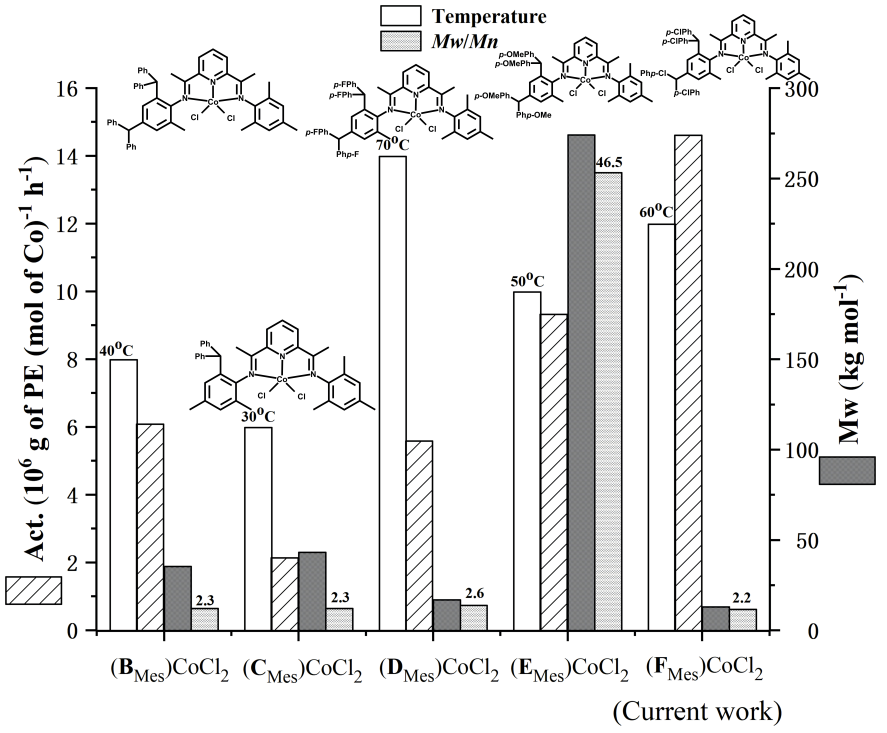

Figure 10. Comparison of thermal stability, catalytic activity, polyethylene molecular weight, and dispersity for $(\mathbf{B}_{Mes})CoCl_2$, $(\mathbf{C}_{Mes})CoCl_2$, $(\mathbf{D}_{Mes})CoCl_2$, and $(\mathbf{E}_{Mes})CoCl_2$ (Chart 1) with the current precatalyst $(\mathbf{F}_{Mes})CoCl_2$ (**Co4**); all polymerization runs were performed at $P_{C_2H_4}$ = 10 atm under their optimal conditions.

linear high-density polyethylene. To corroborate this assertion, two representative samples obtained using **Co1**/MAO at 60 °C (entry 7, Table 2; M_w = 10.4 kg·mol^{-1}) and **Co1**/MMAO at 30 °C (entry 7, Table 3; M_w = 31.5 kg·mol^{-1}) were subjected to high-temperature ^{13}C NMR spectroscopy (recorded at 100 °C in 1,1,2,2-tetrachloroethane-d_2, see Figure 9 and Figure S3). For the sample obtained using **Co1**/MAO at 60 °C, a characteristic singlet resonance at δ 30.00 corresponds to the methylene repeat unit (–CH_2–) for a linear polyethylene [52]; the absence of additional peaks corresponding to chain ends is presumably attributable to the relatively high molecular weight of the sample.

3.4. *Comparison of the current cobalt catalysts with previously reported examples*

To help contextualize the findings in this work, we have extracted key performance data for mesityl-containing **Co4**/MAO [$(\mathbf{F}_{Mes})CoCl_2$] obtained herein (entry 18, Table 2) and assembled this alongside those previously reported for $(\mathbf{B}_{Mes})CoCl_2$, $(\mathbf{C}_{Mes})CoCl_2$, $(\mathbf{D}_{Mes})CoCl_2$, and $(\mathbf{E}_{Mes})CoCl_2$ (Figure 10); all tests were obtained under optimized conditions at $P_{C_2H_4}$ = 10 atm using MAO [47–50]. All five systems are structurally related with $(\mathbf{B}_{Mes})CoCl_2$, $(\mathbf{D}_{Mes})CoCl_2$, $(\mathbf{E}_{Mes})CoCl_2$, and $(\mathbf{F}_{Mes})CoCl_2$ all incorporating *N*-2-Me-4,6-bis(4,4′-X_2dibenzhydryl)phenyl (X = H, F, OMe, Cl) substitution while $(\mathbf{C}_{Mes})CoCl_2$, *N*-2,4-diMe-6-dibenzhydrylphenyl substitution. For the most closely related systems $(\mathbf{B}_{Mes})CoCl_2$, $(\mathbf{D}_{Mes})CoCl_2$, $(\mathbf{E}_{Mes})CoCl_2$, and $(\mathbf{F}_{Mes})CoCl_2$, it is evident that chloro-containing $(\mathbf{F}_{Mes})CoCl_2$ is the most active (14.6×10^6 (g of PE)·(mol of Co)$^{-1}$·h^{-1}; entry 18, Table 2) but forms the lowest molecular weight polymer (M_w = 13.0 kg·mol^{-1}; entry 18, Table 2). Conversely, $(\mathbf{E}_{Mes})CoCl_2$ bearing an electron donating methoxy-substituent showed moderate activity,

but the resulting polyethylene afforded the highest molecular weight (M_w = 274.0 kg·mol^{-1}) and broad dispersity [50]. Evidently, these results underline the electronic influence played by the *para*-groups in the benzhydryl group on catalytic performance. By comparison, ($\mathbf{C}_{Mes}$)$CoCl_2$ showed the lowest activity (2.1×10^6 (g of PE)·(mol of Co)$^{-1}$·h^{-1}) [48], which could be the result of a combination of both steric and electronic effects. Nevertheless, all these classes of benzhydryl-substituted bis(arylimino)pyridyl–cobalt catalyst impart excellent control as evidenced by the single-site-like behavior (M_w/M_n range: 2.2–2.6).

4. Conclusions

In summary, five examples of unsymmetrical 2,6-bis(arylimino)pyridine-cobalt complexes (**Co1**–**Co5**), incorporating one *N*-2,4-bis(di(4-chlorophenyl)methyl)-6-methylphenyl group and one variable *N*-aryl group, have been successfully synthesized from their corresponding free N', N, N''-ligands. All complexes were formed in high yield and fully characterized including by single crystal XRD for **Co1** and **Co2**. Under activation with MAO and MMAO, **Co1**–**Co5** all demonstrated their ability to promote ethylene polymerization with high activities reaching up to 14.74×10^6 (g of PE)·(mol of Co)$^{-1}$·h^{-1} for **Co1**/MAO. Moreover, they could deliver this at an appreciable operating temperature of 60 °C, which is notably higher than that seen in previously reported related examples. Furthermore, the polymerizations are well controlled as is evidenced by narrow molecular-weight distributions. Comparison with a series of structurally related benzhydryl-containing cobalt catalysts highlights the important role of the *para*-chloride group. Overall, this is a rare example of a cobalt-based catalyst system that possesses the combined properties of high thermal stability and high activity producing highly linear polyethylene. This also represents an excellent demonstration of the capacity of rational ligand design to improve the performance of ethylene polymerization catalysts.

Declaration of interests

The authors do not work for, advise, own shares in, or receive funds from any organization that could benefit from this article, and have declared no affiliations other than their research organizations.

Funding

GAS is grateful to the Chinese Academy of Sciences for a President's International Fellowship for Visiting Scientists (grant no. 2025PVB0034).

Underlying data

Supporting information for this article is available on the journal's website under https://doi.org/10.5802/crchim.422 or from the author.

The data underlying the article can be obtained from the corresponding author.

CCDC-2464596 for **Co1** and 2464597 for **Co2** contain the supplementary crystallographic data for this article; these data can be obtained free of charge via http://www.ccdc.cam.ac.uk/conts/retrieving.html.

References

[1] G. J. P. Britovsek, V. C. Gibson, B. S. Kimberley, P. J. Maddox, S. J. McTavish, G. A. Solan, A. J. P. White and D. J. Williams, "Novel olefin polymerization catalysts based on iron and cobalt", *Chem. Commun.* (1998), pp. 849–850.

[2] B. L. Small and M. Brookhart, "Highly active iron and cobalt catalysts for the polymerization of ethylene", *J. Am. Chem. Soc.* **120** (1998), pp. 4049–4050.

[3] G. J. P. Britovsek, M. Bruce, V. C. Gibson, et al., "Iron and cobalt ethylene polymerization catalysts bearing 2,6-bis(imino)pyridyl ligands: Synthesis, structures, and polymerization studies", *J. Am. Chem. Soc.* **121** (1999), pp. 8728–8740.

[4] B. L. Small and M. Brookhart, "Polymerization of propylene by a new generation of iron catalysts: Mechanisms of chain initiation, propagation, and termination", *Macromolecules* **32** (1999), pp. 2120–2130.

[5] G. J. P. Britovsek, V. C. Gibson, B. S. Kimberley, S. Mastroianni, C. Redshaw, G. A. Solan, A. J. P. White and D. J. Williams, "Bis(imino)pyridyl iron and cobalt complexes: the effect of nitrogen substituents on ethylene oligomerisation and polymerisation", *J. Chem. Soc. Dalton Trans.* (2001), pp. 1639–1644.

[6] V. C. Gibson, C. Redshaw and G. A. Solan, "Bis(imino)pyridines: Surprisingly reactive ligands and a gateway to new families of catalysts", *Chem. Rev.* **107** (2007), pp. 1745–1776.

[7] J. Ma, C. Feng, S. Wang, K.-Q. Zhao, W.-H. Sun, C. Redshaw and G. A. Solan, "Bi- and tri-dentate imino-based iron and cobalt pre-catalysts for ethylene oligo-/polymerization", *Inorg. Chem. Front.* **1** (2014), pp. 14–34.

[8] S. D. Ittel, L. K. Johnson and M. Brookhart, "Late-metal catalysts for ethylene homo- and copolymerization", *Chem. Rev.* **100** (2000), pp. 1169–1203.

[9] F. Speiser, P. Braunstein and L. Saussine, "Catalytic ethylene dimerization and oligomerization: Recent developments with nickel complexes containing P,N-chelating ligands", *Acc. Chem. Res.* **38** (2005), pp. 784–793.

[10] C. Bianchini, G. Giambastiani, L. Luconi and A. Meli, "Olefin oligomerization, homopolymerization and copolymerization by late transition metals supported by (imino)pyridine ligands", *Coord. Chem. Rev.* **254** (2010), pp. 431–455.

[11] W.-H. Sun, "Novel polyethylenes via late transition metal complex pre-catalysts", *Adv. Polym. Sci.* **258** (2013), pp. 163–178.

[12] R. Gao, W.-H. Sun and C. Redshaw, "Nickel complex pre-catalysts in ethylene polymerization: new approaches to elastomeric materials", *Catal. Sci. Technol.* **3** (2013), pp. 1172–1179.

[13] S. Wang, W.-H. Sun and C. Redshaw, "Recent progress on nickel-based systems for ethylene oligo-/polymerization catalysis", *J. Organomet. Chem.* **751** (2014), pp. 717–741.

[14] V. C. Gibson and G. A. Solan, in *Topics in Organometallic Chemistry* (Z. Guan, ed.), Springer: Berlin/Heidelberg, 2009, pp. 107–158. Chapter 4.

[15] V. C. Gibson and G. A. Solan, in *Catalysis Without Precious Metals* (R. M. Bullock, ed.), Wiley-VCH: Weinheim, 2010, pp. 111–141.

[16] J. Yu, W. Huang, L. Wang, C. Redshaw and W.-H. Sun, "2-[1-(2,6-Dibenzhydryl-4-methylphenylimino)ethyl]-6-[1-(arylimino)ethyl]-pyridylcobalt(II) dichlorides: Synthesis, characterization and ethylene polymerization behavior", *Dalton Trans.* **40** (2011), pp. 10209–10214.

[17] F. He, W. Zhao, X.-P. Cao, T. Liang, C. Redshaw and W.-H. Sun, "2-[1-(2,6-dibenzhydryl-4-chlorophenylimino)ethyl]-6-[1-aryliminoethyl]pyridyl cobalt dichlorides: Synthesis, characterization and ethylene polymerization behavior", *J. Organomet. Chem.* **713** (2012), pp. 209–216.

[18] S. Wang, W. Zhao, X. Hao, B. Li, C. Redshaw, Y. Li and W.-H. Sun, "2-(1-2,6-Bis[bis(4-fluorophenyl)methyl]-4-methylphenyliminoethyl)-6-[1-(arylimino)ethyl]pyridylcobalt dichlorides: Synthesis, characterization and ethylene polymerization behavior", *J. Organomet. Chem.* **731** (2013), pp. 78–84.

[19] Q. Chen, W. Zhang, G. A. Solan, T. Liang and W. H. Sun, "Methylene-bridged bimetallic bis(imino)pyridine-cobaltous chlorides as precatalysts for vinyl-terminated polyethylene waxes", *Dalton Trans.* **47** (2018), pp. 6124–6133.

[20] R. Zhang, Y. Ma, M. Han, G. A. Solan, Y. Pi, Y. Sun and W.-H. Sun, "Exceptionally high molecular weight linear polyethylene by using N,N,N′-Co catalysts appended with a N′-2,6-bisdi(4-fluorophenyl)methyl-4-nitrophenyl group", *Appl. Organomet. Chem.* **33** (2019), article no. e5157.

[21] Q. Mahmood, Y. Ma, X. Hao and W.-H. Sun, "Substantially enhancing the catalytic performance of bis(imino)pyridylcobaltous chloride pre-catalysts adorned with benzhydryl and nitro groups for ethylene polymerization", *Appl. Organomet. Chem.* **33** (2019), article no. e4857.

[22] J. Yu, H. Liu, W. Zhang, X. Hao and W.-H. Sun, "Access to highly active and thermally stable iron procatalysts using bulky 2-[1-(2,6-dibenzhydryl-4-methylphenylimino)ethyl]-6-[1-(arylimino)ethyl]pyridine ligands", *Chem. Commun.* **47** (2011), pp. 3257–3259.

[23] X. Cao, F. He, W. Zhao, Z. Cai, X. Hao, T. Shiono, C. Redshaw and W.-H. Sun, "2-[1-(2,6-Dibenzhydryl-4-chlorophenylimino)ethyl]-6-[1-(arylimino)ethyl] pyridyl-iron(II) dichlorides: Synthesis, characterization and ethylene polymerization behavior", *Polymer* **53** (2012), pp. 1870–1880.

[24] W. Zhao, J. Yu, S. Song, W. Yang, H. Liu, X. Hao, C. Redshaw and W.-H. Sun, "Controlling the ethylene polymerization parameters in iron pre-catalysts of the type 2-[1-(2,4-dibenzhydryl-6-methylphenylimino)ethyl]-6-[1-(arylimino)ethyl] pyridyliron dichloride", *Polymer* **53** (2012), pp. 130–137.

[25] W.-H. Sun, W. Zhao, J. Yu, W. Zhang, X. Hao and C. Redshaw, "Enhancing the Activity and Thermal Stability of Iron Precatalysts Using 2-(1-2,6-bis[bis(4-fluorophenyl)methyl]-4-methylphenyliminoethyl)-6-[1-(arylimino)ethyl]pyridines", *Macromol. Chem. Phys.* **213** (2012), pp. 1266–1273.

[26] Q. Mahmood, J. Guo, W. Zhang, Y. Ma, T. Liang and W.-H. Sun, "Concurrently improving the thermal stability and activity of ferrous precatalysts for the production of saturated/unsaturated polyethylene", *Organometallics* **37** (2018), pp. 957–970.

[27] Q. Mahmood, E. Yue, J. Guo, W. Zhang, Y. Ma, X. Hao and W.-H. Sun, "Nitro-functionalized bis(imino)pyridylferrous chlorides as thermo-stable precatalysts for linear polyethylenes with high molecular weights", *Polymer* **159** (2018), pp. 124–137.

[28] R. Zhang, M. Han, Y. Ma, G. A. Solan, T. Liang and W.-H. Sun, "Steric and electronic modulation of iron catalysts as a route to remarkably high molecular weight linear polyethylenes", *Dalton Trans.* **48** (2019), pp. 17488–17498.

[29] W.-H. Sun, P. Hao, S. Zhang, Q. Shi, W. Zuo and X. Tang, "Iron(II) and Cobalt(II) 2-(Benzimidazolyl)-6-(1-(arylimino)ethyl)pyridyl complexes as catalysts for ethylene oligomerization and polymerization", *Organometallics* **26** (2007), pp. 2720–2734.

[30] Y. Chen, P. Hao, W. Zuo, K. Gao and W.-H. Sun, "2-(1-Isopropyl-2-benzimidazolyl)-6-(1-aryliminoethyl)pyridyl transition metal (Fe, Co, and Ni) dichlorides: Syntheses, characterizations and their catalytic behaviors toward ethylene reactivity", *J. Organomet. Chem.* **693** (2008), pp. 1829–1840.

[31] L. Xiao, R. Gao, M. Zhang, Y. Li, X. Cao and W.-H. Sun, "2-(1H-2-Benzimidazolyl)-6-(1-(arylimino)ethyl)pyridyl iron(II) and cobalt(II) dichlorides: Syntheses, characterizations, and catalytic behaviors toward ethylene reactivity", *Organometallics* **28** (2009), pp. 2225–2233.

[32] R. Gao, Y. Li, F. Wang, W.-H. Sun and M. Bochman, "2-Benzoxazolyl-6-[1-(arylimino)ethyl]pyridyliron(II) chlorides as ethylene oligomerization catalysts", *Eur. J. Inorg. Chem.* (2009), pp. 4149–4156.

[33] L. Wang, W.-H. Sun, L. Han, H. Yang, Y. Hu and X. Jin, "Late transition metal complexes bearing 2,9-bis(imino)-1,10-

phenanthrolinyl ligands: synthesis, characterization and their ethylene activity", *J. Organomet. Chem.* **658** (2002), pp. 62–70.

[34] W.-H. Sun, S. Jie, S. Zhang, W. Zhang, Y. Song and H. Ma, "Iron complexes bearing 2-Imino-1,10-phenanthrolinyl ligands as highly active catalysts for ethylene oligomerization", *Organometallics* **25** (2006), pp. 666–677.

[35] J. D. A. Pelletier, Y. D. M. Champouret, J. Cardarso, L. Clowes, M. Gañete, K. Singh, V. Thanarajasingham and G. A. Solan, "Electronically variable iminophenanthrolinyl-cobalt complexes; synthesis, structures and ethylene oligomerisation studies", *J. Organomet. Chem.* **691** (2006), pp. 4114–4123.

[36] S. Jie, S. Zhang, K. Wedeking, W. Zhang, H. Ma, X. Lu, Y. Deng and W.-H. Sun, "Cobalt(II) complexes bearing 2-imino-1,10-phenanthroline ligands: synthesis, characterization and ethylene oligomerization", *C. R. Chim.* **9** (2006), pp. 1500–1509.

[37] S. Jie, S. Zhang, W.-H. Sun, X. Kuang, T. Liu and J. Guo, "Iron(II) complexes ligated by 2-imino-1,10-phenanthrolines: Preparation and catalytic behavior toward ethylene oligomerization", *J. Mol. Catal. A* **269** (2007), pp. 85–96.

[38] S. Jie, S. Zhang and W.-H. Sun, "2-Arylimino-9-phenyl-1,10-phenanthrolinyl-iron, -cobalt and -nickel complexes: Synthesis, characterization and ethylene oligomerization behavior", *Eur. J. Inorg. Chem.* (2007), pp. 5584–5598.

[39] J. Guo, W. Zhang, T. Liang and W.-H. Sun, "Revisiting the 2-imino-1,10-phenanthrolylmetal precatalyst in ethylene oligomerization: Benzhydryl-modified cobalt(II) complexes and their dimerization of ethylene", *Polyhedron* **193** (2021), pp. 114865–114873.

[40] Z. Wang, G. A. Solan, W. Zhang and W.-H. Sun, "Carbocyclic-fused N,N,N-pincer ligands as ring-strain adjustable supports for iron and cobalt catalysts in ethylene oligo-/polymerization", *Coord. Chem. Rev.* **363** (2018), pp. 92–108.

[41] C. Bariashir, C. Huang, G. A. Solan and W.-H. Sun, "Recent advances in homogeneous chromium catalyst design for ethylene tri-, tetra-, oligo- and polymerization", *Coord. Chem. Rev.* **385** (2019), pp. 208–229.

[42] F. Huang, Q. Xing, T. Liang, Z. Flisak, B. Ye, X. Hu, W. Yang and W.-H. Sun, "2-(1-Aryliminoethyl)-9-arylimino-5,6,7,8-tetrahydrocycloheptapyridyl iron(II) dichloride: synthesis, characterization, and the highly active and tunable active species in ethylene polymerization", *Dalton Trans.* **43** (2014), pp. 16818–16829.

[43] F. Huang, W. Zhang, E. Yue, T. Liang, X. Hu and W.-H. Sun, "Controlling the molecular weights of polyethylene waxes using the highly active precatalysts of 2-(1-aryliminoethyl)-9-arylimino-5,6,7,8-tetrahydrocycloheptapyridylcobalt chlorides: synthesis, characterization, and catalytic behavior", *Dalton Trans.* **45** (2016), pp. 657–666.

[44] Q. Chen, W. Zhang, G. A. Solan, R. Zhang, L. Guo, X. Hao and W.-H. Sun, "CH(phenol)-bridged Bis(imino)pyridines as compartmental supports for diiron precatalysts for ethylene polymerization: Exploring cooperative effects on performance", *Organometallics* **37** (2018), pp. 4002–4014.

[45] Z. Wang, R. Zhang, W. Zhang, G. A. Solan, Q. Liu, T. Liang and W.-H. Sun, "Enhancing thermostability of iron ethylene polymerization catalysts through N,N,N-chelation of doubly fused α,α′-bis(arylimino)-2,3:5,6-bis(hexamethylene)pyridines", *Catal. Sci. Technol.* **9** (2019), pp. 1933–1943.

[46] C. Bariashir, Z. Wang, Y. Ma, A. Vignesh, X. Hao and W.-H. Sun, "Finely tuned α,α′-Bis(arylimino)-2,3:5,6-bis(pentamethylene)pyridine-based practical iron precatalysts for targeting highly linear and narrow dispersive polyethylene waxes with vinyl ends", *Organometallics* **38** (2019), pp. 4455–4470.

[47] J. Lai, W. Zhao, W. Yang, C. Redshaw, T. Liang, Y. Liu and W.-H. Sun, "2-[1-(2,4-Dibenzhydryl-6-methylphenylimino)ethyl]-6-[1-(arylimino)ethyl] pyridylcobalt(II) dichlorides: Synthesis, characterization and ethylene polymerization behavior", *Polym. Chem.* **3** (2012), pp. 787–793.

[48] S. Wang, B. Li, T. Liang, C. Redshaw, Y. Li and W.-H. Sun, "Synthesis, characterization and catalytic behavior toward ethylene of 2-[1-(4,6-dimethyl-2-benzhydrylphenylimino)ethyl]-6-[1-(arylimino)ethyl]-pyridylmetal (iron or cobalt) chlorides", *Dalton Trans.* **42** (2013), pp. 9188–9197.

[49] W. Zhang, S. Wang, S. Du, C.-Y. Guo, X. Hao and W.-H. Sun, "2-(1-(2,4-Bis((di(4-fluorophenyl)methyl)-6-methylphenylimino)ethyl)-6-(1-(arylimino)ethyl)pyridylmetal (iron or cobalt) complexes: Synthesis, characterization, and ethylene polymerization behavior", *Macromol. Chem. Phys.* **215** (2014), pp. 1797–1809.

[50] S.-F. Yuan, Z. Fan, Y. Yan, Y. Ma, M. Han, T. Liang and W.-H. Sun, "Achieving polydispersive HDPE by N,N,N-Co precatalysts appended with N-2,4-bis(di(4-methoxyphenyl)methyl)-6-methylphenyl", *RSC Adv.* **10** (2020), pp. 43400–43411.

[51] Q. Zhang, Z. Li, M. Han, J. Xiang, G. A. Solan, Y. Ma, T. Liang and W.-H. Sun, "Fluorinated cobalt catalysts and their use in forming narrowly dispersed polyethylene waxes of high linearity and incorporating vinyl functionality", *Catal. Sci. Technol.* **11** (2021), pp. 656–670.

[52] T. Liu, Y. Ma, G. A. Solan, T. Liang and W.-H. Sun, "Exploring ortho-(4,4′-dimethoxybenzhydryl) substitution in iron ethylene polymerization catalysts: Co-catalyst effects, thermal stability, and polymer molecular weight variations", *Appl. Organomet. Chem.* **35** (2021), article no. e6259.

[53] G. M. Sheldrick, "SHELXT – Integrated space-group and crystal-structure determination", *Acta Crystallogr., Sec. A: Found. Adv.* **A71** (2015), pp. 3–8.

[54] G. M. Sheldrick, "Crystal structure refinement with SHELXL", *Acta Crystallogr., Sec. C: Struct. Chem.* **C71** (2015), pp. 3–8.

[55] Q. Zhang, N. Wu, J. Xiang, G. A. Solan, H. Suo, Y. Ma, T. Liang and W.-H. Sun, "Bis-cycloheptyl-fused bis(imino)pyridine-cobalt catalysts for PE wax formation: positive effects of fluoride substitution on catalytic performance and thermal stability", *Dalton Trans.* **49** (2020), pp. 9425–9437.

[56] M. Han, Q. Zhang, I. I. Oleinik, et al., "High molecular weight polyethylenes of narrow dispersity promoted using bis(arylimino) cyclohepta[*b*]pyridine-cobalt catalysts ortho-substituted with benzhydryl & cycloalkyl groups", *Dalton Trans.* **49** (2020), pp. 4774–4784.

[57] M. Han, Q. Zhang, I. I. Oleynik, et al., "Adjusting ortho-cycloalkyl ring size in a cycloheptyl-fused N,N,N-iron catalyst as means to control catalytic activity and polyethylene properties", *Catalysts* **10** (2020), article no. 1002.

[58] M. Han, I. I. Oleynik, Y. Ma, I. V. Oleynik, G. A. Solan, T. Liang and W.-H. Sun, "α,α'-Bis (imino)-2,3:5,6-bis (pentamethylene)pyridines appended with benzhydryl and cycloalkyl substituents: Probing their effectiveness as tunable N,N,N-supports for cobalt ethylene polymerization catalysts", *Appl. Organomet. Chem.* **35** (2021), article no. e6429.

[59] M. Han, I. I. Oleynik, M. Liu, Y. Ma, I. V. Oleynik, G. A. Solan, T. Liang and W.-H. Sun, "Ring size enlargement in an ortho-cycloalkyl-substituted bis(imino)pyridine-cobalt ethylene polymerization catalyst and its impact on performance and polymer properties", *Appl. Organomet. Chem.* **36** (2022), article no. e6429.

[60] Z. Zuo, M. Han, Y. Ma, G. A. Solan, X. Hu, T. Liang and W.-H. Sun, "Fluorinated bis(arylimino)-6,7-dihydro-5H-quinoline-cobalt polymerization catalysts: Electronic versus steric modulation in the formation of vinyl-terminated linear PE waxes", *Appl. Organomet. Chem.* **36** (2022), article no. e6500.

[61] K. F. Tahir, Y. Ma, Q. Mahmood, et al., "Achieving linear α-Macro-olefins in ethylene polymerization through precisely tuned bis(imino)pyridylcobalt precatalysts with steric and electronic parameters", *Precis. Chem.* **2** (2024), pp. 655–668.

[62] Y. Yan, S.-F. Yuan, M. Liu, G. A. Solan, Y. Ma, T. Liang and W.-H. Sun, "Investigating the effects of para-methoxy substitution in sterically enhanced unsymmetrical bis(arylimino)pyridine-cobalt ethylene polymerization catalysts", *Chinese J. Polym. Sci.* **40** (2022), pp. 266–279.

[63] E. Ogbe, Y. Ma, Y. Wang, J. Gao, Y. Sun and W.-H. Sun, "Finely-tuned bis(imino)pyridylcobalt complexes enhance ethylene polymerization: The role of bulky and halogen substituents", *Molecules* **30** (2025), article no. 859.